Thermal analysis of extended surfaces using deep neural networks

Yusuf Olatunji Tijani

Shina Daniel Oloniiju and Olumuyiwa Otegbeye

Department of Mathematics, Rhodes University.

Workshop on Computational Mathematics and Modelling, University of KwaZulu-Natal.
July 4, 2024

Contents

Introduction

Fin (also known as extended surfaces) could be defined as protrusions or appendages deliberately added to the surface of an object to enhance its heat transfer characteristics.

Fins are employed to increase the surface area available for heat exchange, thereby improving the efficiency of cooling or heating processes.

The relevance of fins is evident in our daily lives, influencing cooling processes in refrigerators, the radiator systems in cars, the heating elements in geysers, the thermal fins used in heat dissipation in our computers and numerous other applications around us.

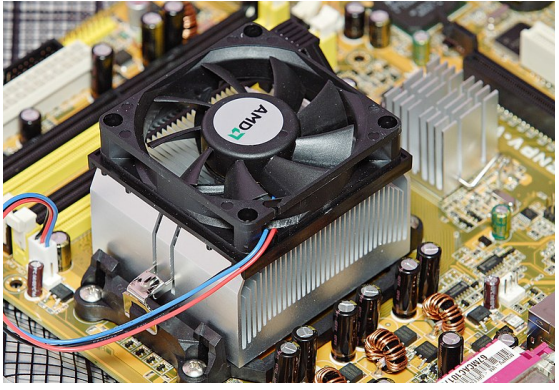

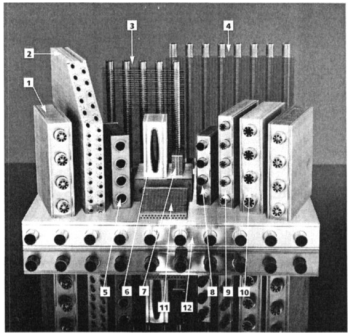

Application of extended surfaces

Literature Review

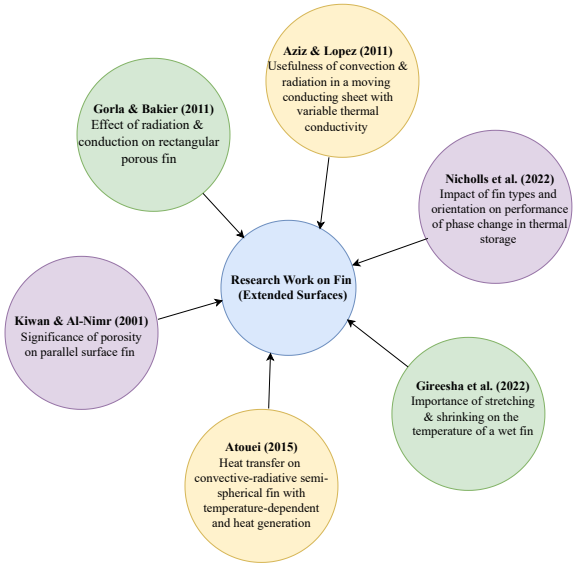


Singha et al. (2015)
Wavelet collocation method on non-linear fin model with variable thermal conductivity
Aderogba et al. (2011)
Non-standard finite difference method on generalized fin model
Oguntola & Hamed (2017)
Haar wavelet method on porous fin with internal heat generation and thermal conductivity
Research Work on Fin (Extended Surfaces)
Kasali et al. (2022)
Spectral local linearization method on multi-boiling rectangular porous fin
Roy et al. (2018)
Modified decomposition method on triangular moving fin
Akindeinde (2018)
Parker-Sochacki method on convective fin with variable thermal conductivity

Model Formulation

The following dynamical cumulative heat equation describes the equilibrium of thermal transport (Kasali et al. 2022, Sobamowo et al. 2018):

$$z(x) = z(x + \delta x) + z_{conv} + z_{rad} + z_{mag} + z_{int} + \text{porous term}. \tag{1}$$

Equation (1) represents the thermal energy balance within a closed system.
The following assumptions are made in deriving the governing equation:

- The porous media is homogeneous and saturates with a single-phase fluid.
- The longitudinal fin is constrained in length with an insulated tip, creating an adiabatic system where no heat is transmitted from the tip.
- The interaction between the porous medium and the single-phase fluid is formulated using the Darcy model.
- The effect of the electrical field due to polarization is considered to be negligible, i.e. $E = 0$.
- Temperature at the base of the fin is $F = F_w$ and at the tip takes the form, $\frac{dF}{dx} = 0$.

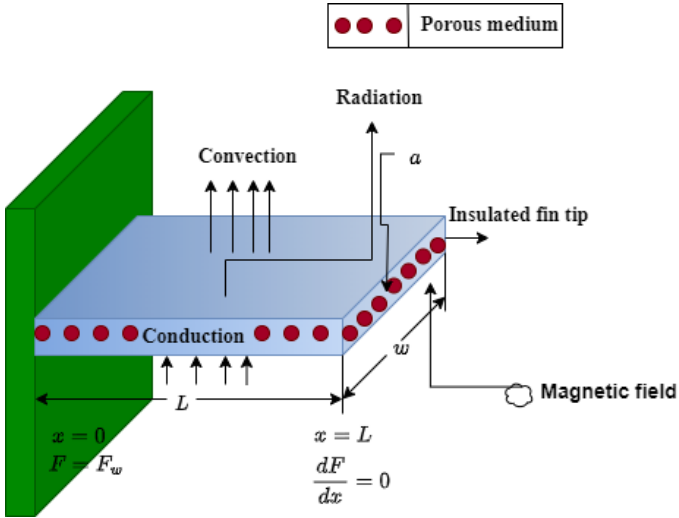

Figure: Geometrical configuration of the fin

$$
\left.
\begin{aligned}
z(x) - z(x+\delta x) \;=\; & \underbrace{\eta(F)(F-F_\infty)\,\delta a}_{\text{heat due to convection}} + \underbrace{\epsilon\sigma_*(F^4-F_\infty^4)\,\delta a}_{\text{heat due to radiation}} \\
+ \; & \underbrace{\frac{J_e \times J_e}{\sigma}\,a\delta x}_{\text{heat due to magnetic element}} + \underbrace{z_{int}(F)\,a\delta x}_{\text{internal heat dissipation}} + \underbrace{\rho c_p w u(x)(F-F_\infty)\,\delta x.}_{\text{heat due to porous effect}}
\end{aligned}
\right\} \tag{2}
$$

Here, $u(x)$ represents the movement of the buoyancy-driven flow at any location x, and J_e is the intensity of the conduction responsible for the thermal transport due to electric current, given, respectively, as (Madhura et al. 2020)

$$
u(x) = \frac{g\beta K}{\nu}(F - F_\infty), \qquad \text{and} \qquad J_e = \sigma(E + V \times B). \tag{3}
$$

Thus,

$$
\left.
\begin{aligned}
z(x) - \left(z(x) + \frac{dz}{dx}\delta x\right) = \; & \eta(F)(F-F_\infty)P\delta x + \epsilon\sigma_*(F^4-F_\infty^4)P\delta x \\
& + \frac{J_e \times J_e}{\sigma}a\delta x + z_{int}(F)a\delta x + \frac{\rho c_p g\beta K}{\nu}w(F-F_\infty)^2\delta x,
\end{aligned}
\right\} \tag{4}
$$

where $\delta a = P\delta x$.

Upon division by δx, and some mathematical adjustment,

$$-\frac{dz}{dx} = \eta(F)P(F - F_\infty) + \epsilon\sigma_* P(F^4 - F_\infty^4) + a\sigma B_0^2 u(x)^2 + a z_{int}(F) + \frac{\rho c_p g \beta K}{\nu} w(F - F_\infty)^2, \quad (5)$$

where $\frac{J_e \times J_e}{\sigma} = \sigma B_0^2 u(x)^2$. Following Fourier's law of heat conduction (Liu 1990), heat conduction taking place within the fin can be mathematically described as,

$$z = -ak(F)\frac{dF}{dx}. \quad (6)$$

$$\left.\begin{aligned}\frac{d}{dx}\left(ak(F)\frac{dF}{dx}\right) &= \eta(F)P(F - F_\infty) + \epsilon\sigma_* P(F^4 - F_\infty^4) \\ &+ a\sigma\frac{B_0^2 g^2 \beta^2 K^2}{\nu^2}(F - F_\infty)^2 + a z_{int}(F) + \frac{\rho c_p g \beta K}{\nu} w(F - F_\infty)^2,\end{aligned}\right\} \quad (7)$$

and using the following relations

$$\left.\begin{aligned} &k(F) = k_a[1 + \alpha_0(F - F_\infty) + \alpha_1^2(F - F_\infty)^2], \quad \eta(F) = \eta_b \left(\frac{F - F_\infty}{F_w - F_\infty}\right)^n, \\ &\text{and} \quad z_{int}(F) = \iota[1 + \xi(F - F_\infty)]. \end{aligned}\right\} \tag{8}$$

After some simplifications, Equation (7) becomes

$$\left.\begin{aligned} &\frac{d}{dx}\left[k_a[1 + \alpha_0(F - F_\infty) + \alpha_1^2(F - F_\infty)^2]\frac{dF}{dx}\right] - \frac{\eta_b P(F - F_\infty)^{n+1}}{a(F_w - F_\infty)^n} - \frac{\epsilon\sigma_* P}{a}(F^4 - F_\infty^4) \\ &\quad - \iota[1 + \xi(F - F_\infty)] - \frac{\sigma B_0^2 g^2 \beta^2 K^2}{\nu^2}(F - F_\infty)^2 - \frac{\rho c_p g \beta K w}{a}(F - F_\infty)^2 = 0, \end{aligned}\right\} \tag{9}$$

with associated boundary conditions given as

$$\left.\begin{aligned} &\text{at} \quad x = 0, \quad F = F_w, \\ &\text{at} \quad x = L, \quad \frac{dF}{dx} = 0. \end{aligned}\right\} \tag{10}$$

We now introduce the following dimensionless variables and parameters:

$$\left.\begin{aligned}
&\zeta = \frac{x}{L}, \quad \Gamma = \frac{F - F_\infty}{F_w - F_\infty}, \quad M = \frac{\eta_b P L^2}{a k_a}, \quad Q = \frac{\iota L^2}{k_a (F_w - F_\infty)}, \quad \phi_0 = \alpha_0 (F_w - F_\infty), \\
&\phi_1 = \alpha_1^2 (F_w - F_\infty)^2, \quad N_P = \frac{\rho c_p g \beta K w L^2 (F_w - F_\infty)}{a \nu k_a}, \quad N_R = \frac{L^2 \sigma_* P (F_w - F_\infty)^3}{a k_a}, \\
&N_F = \frac{F_\infty}{F_w - F_\infty}, \quad \xi_* = \xi (F_w - F_\infty), \quad H = \frac{\sigma B_0^2 g^2 \beta^2 K^2 L^2 (F_w - F_\infty)}{\nu^2 k_a}.
\end{aligned}\right\} \tag{11}$$

We obtained the following single variable differential equation:

$$\frac{d}{d\zeta}\left[K_1(\Gamma)\frac{d\Gamma}{d\zeta}\right] - M\Gamma^{n+1} - \epsilon N_R\left[(N_F + \Gamma)^4 - N_F^4\right] - (H + N_P)\Gamma^2 - Q\,(1 + \xi_*\Gamma) = 0, \tag{12}$$

where $K_1(\Gamma) = 1 + \phi_0\Gamma + \phi_1\Gamma^2$ and its associated insulated boundary conditions

$$\text{at} \quad \zeta = 0, \ \Gamma = 1, \quad \text{and} \quad \text{at} \quad \zeta = 1, \ \frac{d\Gamma}{d\zeta} = 0. \tag{13}$$

The fin efficiency is computed by dividing the rate of heat transfer (Z_{fin}) by the ideal rate of heat transfer (Z_{ideal}), where the latter represents the thermal energy that would be conducted if the entire fin temperature were the same as the temperature of the fin base. This relationship is expressed as (Madhura et al. 2020):

$$Z_r = \frac{Z_{fin}}{Z_{ideal}} = \frac{\int_0^L P(F - F_\infty)dx}{PL(F_w - F_\infty)} = \int_0^1 \Gamma(\zeta)d\zeta, \tag{14}$$

where $Z_{fin} = \int_0^L P(F - F_\infty)dx$ is the rate of heat transfer.

Numerical Method

This study uses a deep and fully connected feedforward artificial neural networks framework to solve the nonlinear differential equation (12) with the associated boundary conditions (13). Suppose the differential equation (12) is defined as

$$\mathcal{G}\left[\zeta, \Gamma(\zeta), \frac{\mathrm{d}\Gamma(\zeta)}{\mathrm{d}\zeta}, \frac{\mathrm{d}^2\Gamma(\zeta)}{\mathrm{d}\zeta^2}\right] = 0, \qquad \zeta \in [0,1], \tag{15}$$

subject to the conditions in (13), where $\mathcal{G}$ is a nonlinear operator of $\Gamma(\zeta)$ and its derivatives.

- The set of Chebyshev-Gauss-Lobatto points,

$$\tilde{\zeta}_{\mathsf{j}} = -\cos\left(\frac{\pi \mathsf{j}}{\mathsf{M}_\zeta}\right), \quad \mathsf{j} = 0, \ldots, \mathsf{M}_\zeta,$$

  mapped onto $\zeta \in [0,1]$.
- The nonlinear differential equation (15) is then transformed into its discrete equivalent

$$\mathcal{G}\left[\zeta_{\mathsf{j}}, \Gamma(\zeta_{\mathsf{j}}), \frac{\mathrm{d}\Gamma(\zeta_{\mathsf{j}})}{\mathrm{d}\zeta}, \frac{\mathrm{d}^2\Gamma(\zeta_{\mathsf{j}})}{\mathrm{d}\zeta^2}\right] = 0, \qquad \zeta_{\mathsf{j}} \in \frac{1}{2}(\tilde{\zeta}+1) \equiv [0,1], \tag{16}$$

  subject to the conditions

$$\Gamma(\zeta_0) = 1 \quad \text{and} \quad \frac{\mathrm{d}\Gamma(\zeta_{M_\zeta})}{\mathrm{d}\zeta} = 0. \tag{17}$$

Consider the ansatz, $\Gamma_t(\zeta; w, b)$, which satisfies the boundary conditions (17) for the solution of the differential equation (16). Here, w and b are the weights and biases of the deep neural networks framework. Therefore, the problem of approximating the solution of the differential equation then becomes the unconstrained minimization problem,

$$\min_{w,b} \sum_{\zeta_j \in [0,1]} \left(\mathcal{G}\left[\zeta_j, \Gamma_t(\zeta_j; w, b), \frac{\mathrm{d}\Gamma_t(\zeta_j; w, b)}{\mathrm{d}\zeta}, \frac{\mathrm{d}^2\Gamma_t(\zeta_j; w, b)}{\mathrm{d}\zeta^2} \right] \right)^2. \tag{18}$$

In the proposed technique, the trial solution, $\Gamma_t(\zeta; w, b)$, is defined as

$$\Gamma_t(\zeta; w, b) = 1 + \zeta \left(N(\zeta; w, b) - N(1; w, b) - \frac{\mathrm{d}N(1; w, b)}{\mathrm{d}\zeta} \right). \tag{19}$$

The trial solution, $\Gamma_t(\zeta; w, b)$, depends on the output, $N(\zeta; w, b)$, of the neural networks framework and is chosen to satisfy the boundary conditions, (13), of the differential model.

$\mathrm{N}(\zeta; \mathrm{w}, \mathrm{b})$ is the single output of a feedforward deep neural network architecture fed with a single input vector, ζ_{j}.

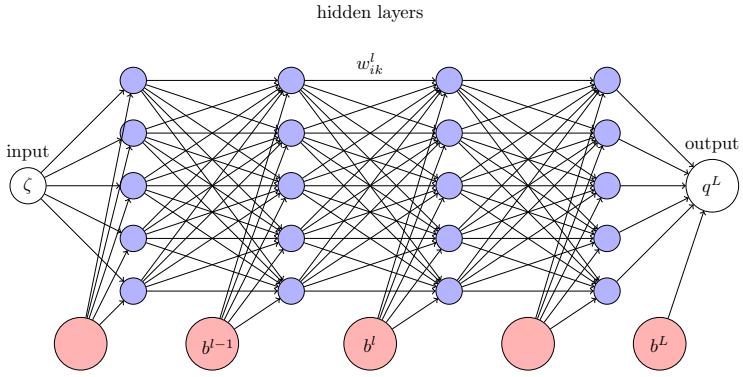

Figure: Schematic diagram of a fully connected deep neural network.

- The sigmoid activation function, $\varrho(\mathrm{q}) = (1 + \mathrm{e}^{-\mathrm{q}})^{-1}$, is used.

- The neural network framework is expressed mathematically as follows:

$$\left.\begin{aligned} q^0 &= \zeta, && \text{the input layer} \\ q^l &= \varrho^l(w^l q^{l-1} + b^l), \quad 1 < l < L-1, && \text{the hidden layers} \\ q^L &= w^L q^{L-1} + b^L, && \text{the output layer,} \end{aligned}\right\} \tag{20}$$

  where the result of the output layer, $q^L = N(\zeta; w, b)$, is used in the trial solution (19).

- To find the weights and biases in the layers, we minimize the residual function

$$\mathcal{R}(w, b) = \sum_{j=0}^{M_\zeta} \left(\mathcal{G}\left[\zeta_j, \Gamma_t(\zeta_j; w, b), \frac{d\Gamma_t(\zeta_j; w, b)}{d\zeta}, \frac{d^2\Gamma_t(\zeta_j; w, b)}{d\zeta^2} \right] \right)^2, \tag{21}$$

  using gradient descent optimization with adaptive moment estimation.

We used the GradientTape sub-module of Python's TensorFlow package. The weights and biases are then updated through backward propagation. The neural network is completely implemented with Python programming language using the TensorFlow and NumPy packages.

During the training process, the network adjusts its parameters, viz weights and biases, to minimize the loss and improve the predictability of the trial solution.

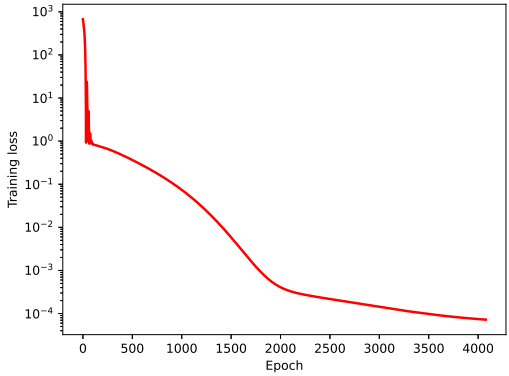

Figure: Training loss curve of the neural networks algorithm with six hidden layers and 50 neurons in each hidden layer.

Table: Step-by-step algorithm for solving Equation (12) using a fully connected deep neural network.

1. Define the variable $\mathsf{q}^0 = \zeta$ as input.
2. Define the number of hidden layers and number of neurons in each layer.
3. Initialize the weights and biases for each layer and set them as trainable parameters.
4. Define the neural networks architecture:
5. **for** $\mathsf{l} = 1$ **to** L
6. $\mathsf{q}^{\mathsf{l}} = \varrho^{\mathsf{l}}(\mathsf{w}^{\mathsf{l}}\mathsf{q}^{\mathsf{l}-1} + \mathsf{b}^{\mathsf{l}})$ **end for**
7. Define the trial solution: $\Gamma_{\mathsf{t}}(\zeta; \mathsf{w}, \mathsf{b}) = 1 + \zeta\,(\mathsf{N}(\zeta; \mathsf{w}, \mathsf{b}) - \mathsf{N}(1; \mathsf{w}, \mathsf{b}) - \mathsf{N}'(1; \mathsf{w}, \mathsf{b}))$.
8. Define the loss function $\mathcal{R}(\mathsf{w}, \mathsf{b})$ in (21) in terms of the trial function.
9. Define the model parameters, $\phi_0, \phi_1, \mathsf{M}, \mathsf{n}, \epsilon, \mathsf{N}_{\mathsf{R}}, \mathsf{N}_{\mathsf{F}}, \mathsf{H}, \mathsf{N}_{\mathsf{P}}, \mathsf{Q}, \xi_*$ as untrainable parameters.
10. Train the neural network model to optimize the weights and biases by minimizing the residual function.

Remark

The spectral local linearization method for Equation (12), given the conditions specified in Equation (13), is implemented for validation purposes.

Results and Discussion

The goal of this study is in two folds:

- to develop a deep neural network for simulating the fin dynamical model
- to investigate the impacts of each dimensionless parameter, since the model is novel.

Hence, If not specified otherwise, the analysis of the results was carried out using the following parameter values: $\mathrm{M} = 1.0,\ \mathrm{N_R} = 0.10,\ \mathrm{N_F} = 0.10,\ \mathrm{n} = 1.0,\ \epsilon = 1.0,\ \phi_0 = 0.10,\ \phi_1 = 0.30, \mathrm{N_P} = 1.0,\ \mathrm{H} = 1.0,\ \mathrm{Q} = 0.2$, and $\xi_* = 1.0$.

Validation of the method

Table: The fin efficiency rate as computed using the deep neural network approach and the spectral local linearization method with the following values: $\mathrm{N_R} = 0.10,\ \mathrm{n} = 1.0,\ \mathrm{N_F} = 0.10, \mathrm{Q} = \phi_0 = \phi_1 = 0.0$, $\xi_* = 0.6$ and $\epsilon = 1.0$.

M	H	$\mathrm{N_P}$	DNN	SLLM
1.0	0.5	2.0	0.62475	0.62495
2.0	–	-	0.58602	0.58633
1.0	0.1	2.0	0.64334	0.64352
–	0.3	–	0.63385	0.63397
1.0	0.5	1.0	0.67598	0.67612
–	–	1.5	0.64839	0.64852

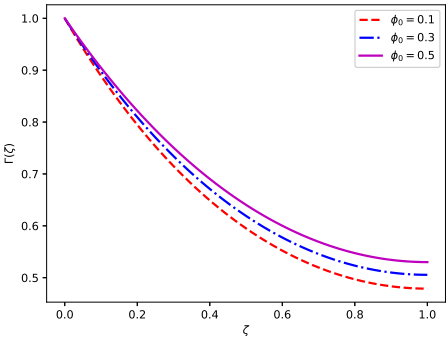

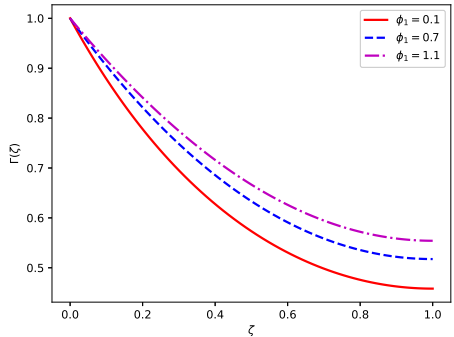

Figure: The impacts of linear (ϕ_0), and nonlinear (ϕ_1), thermal conductivity on temperature of the fin.

The linear relationship suggests that the thermal conductivity of the fin changes uniformly with temperature. On the other hand, the nonlinear thermal conductivity variation has a much more complex, non-uniform or even non-monotonic relationship with the temperature.

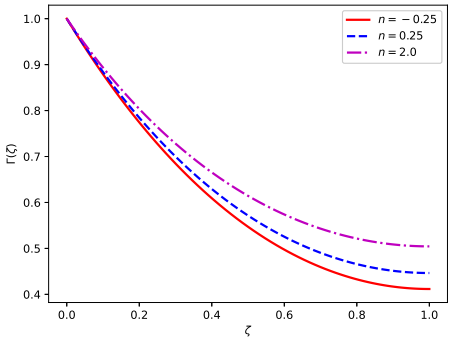

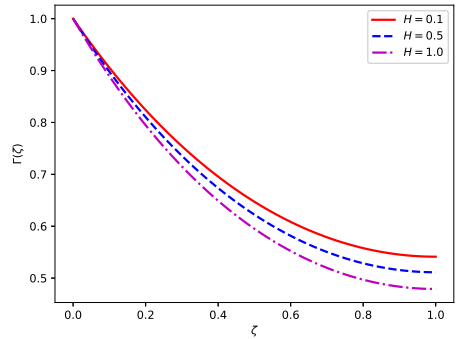

Figure: The impacts of multi-boiling (n) and magnetic parameter (H) on the temperature of the fin.

$n = -\frac{1}{4}$ indicates laminar film boiling, natural convection corresponds to $n = \frac{1}{4}$, and $n = 2$ represents nucleate boiling. Increasing the magnetic field parameter has a notable effect on the temperature distribution at the tip of the fin. As the parametric value of the magnetic field parameter increases, the temperature at the tip decreases.

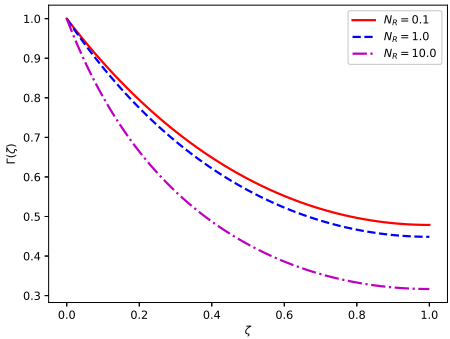

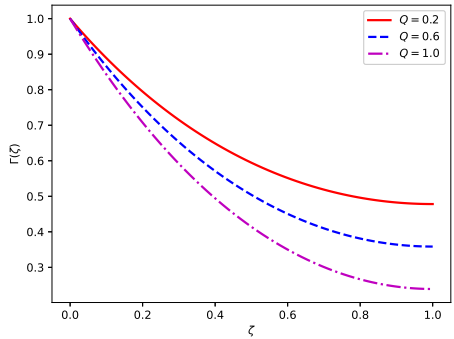

Figure: The impacts of radiation (N_R) and internal heat generation (Q) on the temperature of the fin.

Increasing the thermal radiation parameter reduces the temperature observed on the extended surface. This phenomenon arises because enhanced thermal radiation facilitates heat transfer away from the surface. A significant decrease in the temperature of the fin at its tip is experienced as the fin generates more internal heat.

Conclusion

Novelty

The primary objective of this study is to develop a deep learning algorithm for approximating the solution of a differential equation that describes the intricate dynamics of heat transfer on extended surfaces.

The study also seeks to elucidate the physical implications of some physical parameters arising from the differential model.

Methodology

A deep neural network architecture was designed to approximate the solution of the differential model. The loss function was used to assessed our stopping criterion and to check convergence of the method.

A spectral-based numerical method was used to benchmark the result of the neural network technique.

Findings

It was observed that variations in the thermal radiation parameter exert a comparable influence on reducing the fin temperature at the tip when compared to changes in the internal heat generation parameters.

Using materials with varying thermal conductivity can enhance the efficiency of an extended surface, thus optimizing the heat transfer process.

References

1. R. S. R. Gorla and A. Y. Bakier. Thermal analysis of natural convection and radiation in porous fins. International Communications in Heat and Mass Transfer, 38(5):638–645, 2011.
2. S. Kiwan and M. Al-Nimr. Enhancement of heat transfer using porous fins. ASME Journal of Heat Transfer, 123(4):790–795, 2001.
3. I. E Lagaris, A. Likas, and D. I. Fotiadis. Artificial neural networks for solving ordinary and partial differential equations. IEEE Transactions on Neural Networks and Learning Systems, 9(5):987–1000, 1998.
4. P. K. Roy, A. Mallick, H. Mondal, and P. Sibanda. A modified decomposition solution of triangular moving fin with multiple variable thermal properties. Arabian Journal for Science and Engineering, 43(2):1485–1497, 2018.
5. A. A. Aderogba, O. O. Fabelurin, S. O. Akindeinde, A. O. Adewumi, and B. S. Ogundare. Nonstandard finite difference approximation for a generalized fins problem. Mathematics and Computers in Simulation, 178:183–191, 2020.
6. K. B. Kasali, S. O. Akindeinde, Y. O. Tijani, A. O. Adewumi, and R. S. Lebelo. Thermal and multi-boiling analysis of a rectangular porous fin: A spectral approach. Nonlinear Engineering, 11(1):654–663, 2022.

RHODES UNIVERSITY
Where leaders learn

Thank you.
Questions?

Thermal analysis of extended surfaces using deep neural networks
July 4, 2024